

NJC

New Journal of Chemistry

Accepted Manuscript

A journal for new directions in chemistry

This article can be cited before page numbers have been issued, to do this please use: A. Das, A. Nagaraj, V. Perumal, A. Dhakshinamoorthy and S. Biswas, *New J. Chem.*, 2020, DOI: 10.1039/D0NJ01891K.



This is an Accepted Manuscript, which has been through the Royal Society of Chemistry peer review process and has been accepted for publication.

Accepted Manuscripts are published online shortly after acceptance, before technical editing, formatting and proof reading. Using this free service, authors can make their results available to the community, in citable form, before we publish the edited article. We will replace this Accepted Manuscript with the edited and formatted Advance Article as soon as it is available.

You can find more information about Accepted Manuscripts in the [Information for Authors](#).

Please note that technical editing may introduce minor changes to the text and/or graphics, which may alter content. The journal's standard [Terms & Conditions](#) and the [Ethical guidelines](#) still apply. In no event shall the Royal Society of Chemistry be held responsible for any errors or omissions in this Accepted Manuscript or any consequences arising from the use of any information it contains.

Journal Name

ARTICLE

A Hydrazine Functionalized UiO-66(Hf) Metal-Organic Framework for the Synthesis of Quinolines by Friedländer Condensation

 Aniruddha Das,^{a§} Nagaraj Anbu,^{b§} Perumal Varalakshmi,^c Amarajothi Dhakshinamoorthy^{*b} and Shyam Biswas^{*a}

 Received 00th January 20xx,
Accepted 00th January 20xx

DOI: 10.1039/x0xx00000x

www.rsc.org/

A hydrazine functionalized Hf-UiO-66 metal-organic framework (MOF) (called **1**) was prepared by traditional solvothermal method and it was characterized completely. The material showed high chemical stability in various solvent systems. The activated material (called **1'**) was successfully employed as a solid heterogeneous catalyst for the synthesis of quinolone scaffold in the modified Friedländer synthesis. The catalyst is able to produce 95% yield of the product 3-acetyl-2,4-dimethylquinoline through Friedländer condensation of 2-aminoacetophenone and acetylacetone as starting materials at 100 °C. It also exhibited broad substrate scope in this catalytic reaction. Various control experiments were carried out with respect to the activity of the presented catalyst which clearly indicated its active role. The stability and recyclability of the catalyst were also examined. A series of control experiments for this catalysis has shown that the Lewis acidic metal nodes and Brønsted acidic –NHNH₂ functional group of linker play the active roles in the catalysis.

Introduction

Quinolines are an important class of heterocyclic compounds because of their anti-tuberculosis, anti-bacterial, anti-HIV, anti-malarial and anti-cancer activities.¹⁻⁵ Many biologically active natural products, especially alkaloid compounds, contain the quinoline scaffolds.⁶⁻⁹ Furthermore, they are used as ligands for the preparation of various metal-complexes.¹⁰ Thus, the development of new synthetic approaches for quinoline and its derivatives is very appealing to chemists.¹¹ Consequently, new synthetic methodologies such as Skraup–Doebnervon Miller,¹² Pfitzinger,^{13, 14} Combes reaction,¹⁵ and Friedländer have been developed for the synthesis of quinoline ring based compounds. The Friedländer reaction is a condensation reaction between 2-aminoaryl ketones and β-ketoesters/ketones possessing reactive α-methylene groups.¹ Substitution in quinoline scaffolds by alkynes, alkenes, alcohols, 2-aminoaryl methanols, 2-iodoanilines and 2-nitroaryl aldehydes has been developed by modified Friedländer synthesis and the modification can affect the

biological activity of the final products.^{16, 17} Although few reaction protocols such as hetero-Diels-Alder reaction of azadiene,¹⁸ and transition-metal-catalyzed¹⁷ reactions have been studied for the synthesis of quinoline scaffolds, it is still highly challenging to incorporate various alkyl moieties at C-4 positions of quinoline scaffold in more efficient and straightforward way. For the preparation of quinoline based heterocyclic compounds, the Friedländer reaction is highly preferred due its mild reaction conditions and high yield. Up to date, the Friedländer and modified Friedländer synthesis have been catalyzed by Basolite™C300, CuBTC,² SO₃H-functionalized ionic liquid,¹⁹ Ag-Pd/C alloy nanoparticle,²⁰ Mn(I) PNP complex,²¹ pincer complexes,²² trifluoroacetic acid-immobilized Fe₃O₄@SiO₂-APTES,²³ etc. The existing catalysts have many shortcomings such as requirement of highly acidic and/or oxidizing media, high temperatures, long reaction times, harmful organic solvents, expensive metal catalysts and large amount of metal salts. These drawbacks drive the necessity of developing new catalysts.²⁴

Due to their versatile structural and chemical properties, metal-organic frameworks (MOFs) are considered as one of the most promising class of materials. Over last two decades, highly crystalline MOFs have gained much scientific attention due to their several unique features such as gas storage and separation, chemical sensing, optoelectronic devices, drug delivery, proton conductivity, etc.²⁵⁻²⁹ The high surface area, considerable thermal and chemical stability along with uniform distribution of pore channels inside the MOFs make them suitable candidates for heterogeneous catalysis for a variety of organic transformation reactions.³⁰⁻³² In the last few years, Zr/Hf based MOFs have been established as pioneering MOF based heterogeneous catalysts due to their unique properties

^a Department of Chemistry, Indian Institute of Technology Guwahati, 781039 Assam, India. Phone: 91-3612583309, Fax: 91-3612582349, E-mail: sbiswas@iitg.ac.in

^b School of Chemistry, Madurai Kamaraj University, Madurai 625021, Tamil Nadu, India. E-mail: admguru@gmail.com

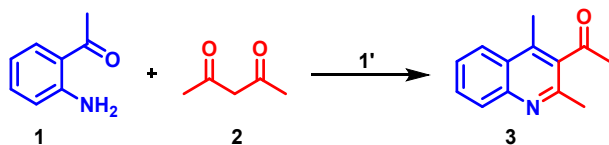
^c Department of Molecular Microbiology, School of Biotechnology, Madurai Kamaraj University, Madurai, Tamil Nadu 625021, India.

§Both are first authors

†Electronic Supplementary Information (ESI) available: Materials and characterization methods, IR spectra, EDX spectra and images, FE-SEM images, TG curves, N₂ sorption isotherms, pore-size distribution curve, XRPD patterns, GC-MS traces and ¹H NMR spectra. See DOI: 10.1039/x0xx00000x

such as extraordinary thermal, chemical and mechanical stability, dual active sites and recyclability performances.³³⁻³⁷ The Friedländer quinoline synthesis is basically catalyzed by Lewis or Brønsted acids.^{9, 38, 39} In this regard, Hf MOFs are more suitable candidates as catalysts because of their more oxophilic character or greater charge separation as $M^{n+}-O^{2-}$.^{40, 41} The catalytically active site might be located at the Hf nodes or at the linker. In addition, the UiO-66 MOFs generally contain some defects (missing linker/missing cluster type) which also promote the catalytic performances of the MOFs.^{40, 42-45}

The main objective of this work is to check the role of Lewis acidic (LA) metal nodes and Brønsted acidic (BA) $-NHNH_2$ functional moiety attached to the linker body in the modified Friedländer synthesis of quinolines. Herein, we report the catalytic performances of Hf-UiO-66- N_2H_3 MOF in the synthesis of 1-(2,4-dimethylquinolin-3-yl)ethan-1-one from 1-(2-aminophenyl)ethan-1-one and acetylacetone. The catalyst showed wide substrate scopes for the synthesis of a series of substituted quinolines. The catalyst is highly stable and recyclable towards the catalysis. The detailed experimental study showed that both the LA and BA centers present in the framework play crucial roles in the formation of quinoline scaffolds. The roles of free linker as well as metal salt were also checked during the catalysis.



Scheme 1. Reaction scheme for the Friedländer condensation between substrate **1** and substrate **2** yielding product **3** using **1'** as solid catalyst.

EXPERIMENTAL SECTION

Synthesis of $[Hf_6O_4(OH)_4(BDC-N_2H_3)_6] \cdot 6H_2O \cdot 7DMF$ (Hf-UiO-66- N_2H_3 , compound **1**)

Reaction of a mixture of $HfCl_4$ (66 mg, 0.204 mmol), $H_2BDC-N_2H_3$ linker (40 mg, 0.204 mmol) and formic acid (769 μ L, 6.12 mmol) in *N,N*-dimethylformamide (DMF; 3 mL) resulted in a light yellow precipitate when the reaction mixture was allowed to heat inside a sealed tube using a pre-heated aluminum heating block for one day at 120 °C. After filtering the precipitate, it was washed with acetone several times. The drying of the powder sample was accomplished at 60 °C in an oven for 4 h. Yield: 80 mg (0.03 mmol, 97%) considering $HfCl_4$. IR (KBr, cm^{-1}): 3435 (br), 1681 (m), 1650 (w), 1621 (w), 1583 (vs), 1503 (m), 1432 (m), 1393 (s), 1305 (m), 1268 (w), 1159 (w), 1100 (w), 1017 (m), 973(m), 769 (s), 748 (w), 676 (vs), 552 (w), 476 (s).

Activation of compound **1**

After stirring compound **1** (100 mg) in methanol (30 mL) at ambient temperature over 24 h, its methanol-exchanged form was obtained. After that the drying of the compound was performed at 80 °C in an oven for 6 h. The activated form of **1** (called **1'**) was obtained after heating this powder sample at 120 °C in high vacuum for one day.

Reaction procedure for catalysis study

In a typical procedure, 2-aminoacetophenone (**1**, 0.5 mmol) and acetylacetone (**2**, 0.3 mL) were added into the reaction vessel comprising 25 mg of **1'**. Then, this heterogeneous mixture was uniformly mixed and placed in an oil bath after reaching the oil temperature to 100 °C. The product formation was monitored using Agilent 7820A gas chromatography by means of taking samples periodically from the reaction mixture. The observed product was identified by GC-MS and 1H -NMR methods (Figs. S12-S31, ESI⁺). After prescribed reaction duration the catalyst was washed two to three times with fresh methanol followed by drying at 80 °C for 3 h. Finally, this dried MOF catalyst was reemployed in the next cycle of Friedlander condensation between fresh 2-aminoacetophenone and acetylacetone. A similar experimental condition was followed for each recycles. An analogous experimental procedure was employed for the optimization studies with respect to catalyst dosage (10, 20, 25 and 30 mg), reaction temperature (60, 80, 100 and 120 °C) and pyridine (50 wt% with respect to **1'**) poison test. The catalytic experiment with the free linker (10 mg, 40.57 wt%) was performed with identical loading of the linker in **1'** under analogous experimental conditions as described above.

Results and discussion

Preparation and activation procedure

The synthesis and activation of catalyst **1** were performed following the procedure previously reported by us.⁴¹ Compound **1** was subjected to activation as described in the Experimental section to remove solvents from the voids and named as **1'**. Later, compound **1'** was used for catalytic experiments.

Characterization

Although the synthesis and characterization of the catalyst have been reported,⁴¹ still for better clarification, we have further characterized the catalyst using XRPD, FT-IR, EDX and FE-SEM analyses. The XRPD pattern (Fig. 1) shows that the catalyst is formed in pure phase with excellent crystallinity. The FT-IR spectra (Fig. S1, ESI⁺) also reveal that there are peaks at 1586 cm^{-1} and 1429 cm^{-1} due the asymmetric and symmetric stretching vibrations of carboxylates of the BDC- N_2H_3 linkers.

The peak at 1660 cm^{-1} is present in the FT-IR spectrum of **1** (Fig. S1, ESI[†]) due to the presence of DMF molecules but this peak is absent in **1'** which confirmed the complete activation of compound **1**. The EDX elemental spectrum and mapping analyses (Figs. S2-S5, ESI[†]) confirmed the presence of Hf, C, O and N atoms in the framework of the catalyst. Moreover, the octahedral shape of the catalyst particles was confirmed by the FE-SEM analysis (Figs. S6-S7, ESI[†]). All these results are consistent with our previously reported results.⁴¹ In our previous study of TG analysis (Fig. S8, ESI[†]), it was observed that both the as-synthesized as well as activated material are thermally stable up to $400\text{ }^{\circ}\text{C}$. The BET surface area and pore-volume of the activated material towards N_2 sorption experiment were $1303\text{ m}^2\text{ g}^{-1}$ and $0.74\text{ cm}^3\text{ g}^{-1}$ (at $p/p_0 = 0.5$), respectively (Fig. S9, ESI[†]). The pore size distribution curve (Fig. S10, ESI[†]) shows that the micropores are centered at 15.4 \AA .

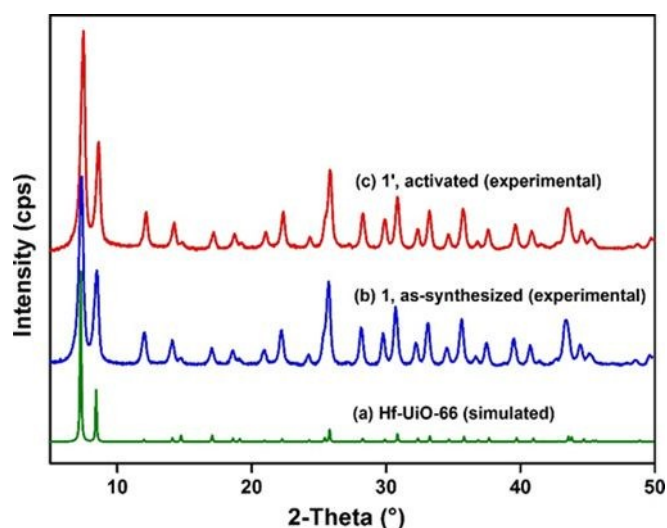


Fig. 1 (a) Theoretical XRPD pattern of Hf-UiO-66 and observed XRPD patterns of (b) **1** and (c) **1'**.

Chemical stability

The chemical stability of the catalyst was checked in different solvent systems. In our previous work,⁴¹ the chemical stability was checked in water, 1 M HCl and glacial acetic acid for 4 h only. However, in the present work, the chemical stability was checked for longer time (24 h) as compared to the previous report (4 h). The XRPD patterns (Fig. S11, ESI[†]) of the solids recovered after stirring in the above-stated solvents were recorded and the data confirmed that the catalyst is stable enough in these three solvent systems over a period of 24 h.

Structure description

The structural description was provided in our previous report.⁴¹ A brief description is provided here. The secondary building unit (SBU) of the MOF catalyst is composed of $[\text{Hf}_6\text{O}_4(\text{OH})_4]^{12+}$ units and the coordination geometry of Hf is square anti-prismatic. Each hexanuclear SBU is connected to adjacent SBUs by twelve BDC- N_2H_3 linkers. The framework structure of the catalyst has larger octahedral and smaller tetrahedral porous cages.

Catalytic activity in Friedländer reaction

The catalytic performance of **1'** was investigated in the synthesis of 3-acetyl-2,4-dimethylquinoline (**3**) (Scheme 1) through Friedländer condensation of **1** and **2** as starting materials at $100\text{ }^{\circ}\text{C}$. The Friedländer condensation between **1** and **2** in the absence of solid catalyst showed no product formation. On other hand, this condensation in the presence of **1'** exhibited quantitative conversion of **1** towards the expected product at $100\text{ }^{\circ}\text{C}$ after 20 h. Fig. 2 shows the time conversion plot for the condensation with and without solid catalyst. Under these reaction conditions, leaching experiment was performed to ascertain the heterogeneity of the process. The progress of the reaction was completely stopped upon removal of the solid from the reaction mixture as shown in Fig. 2. These results suggest that the reaction is promoted by the presence of solid catalyst and no metal ions are leached into the solution, thus proving the heterogeneity of the catalysis. Further, the filtrate was subjected to ICP-AES and no metal ions were observed, which further confirms the stability of the solid catalyst under these reaction conditions.

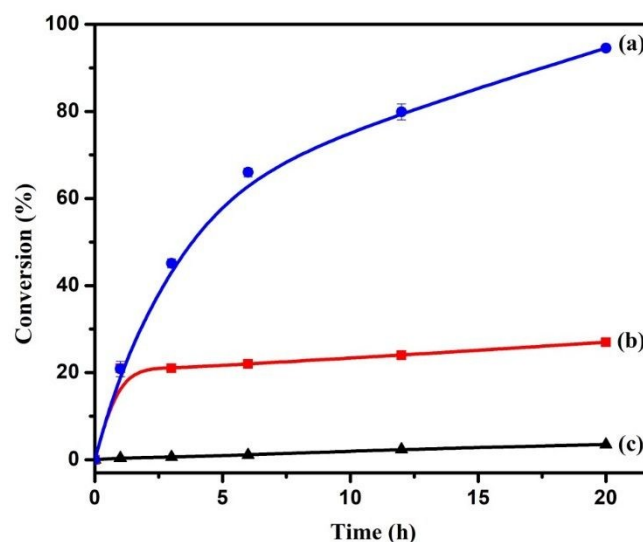


Fig. 2 Time conversion plots for the Friedländer condensation between substrate **1** and substrate **2** (a) in the presence of catalyst **1'**, (b) catalyst filtered after 1 h from the reaction mixture and (c) blank experiment in the absence of catalyst.

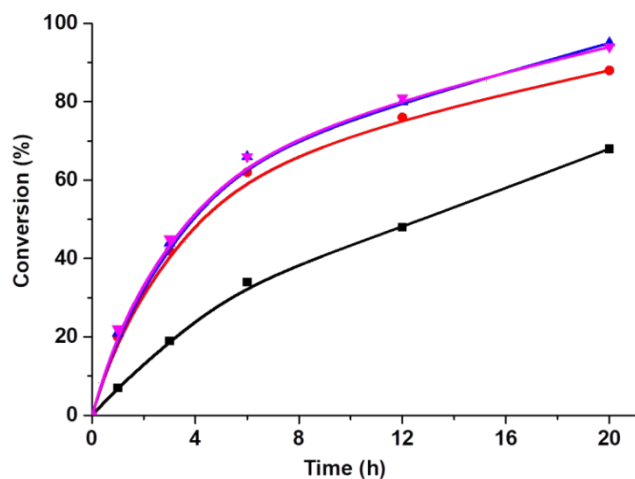


Fig. 3 Effect of catalyst loading for the Friedländer condensation between substrate **1** and substrate **2** at (■) 10 mg, (●) 20 mg, (▼) 25 mg and (▲) 30 mg. The conversions are average of two independent experiments.

Fig. 3 indicates the effect of catalyst dosage on the rate of the reaction in terms of product formation. The desired product was enhanced upon gradual increase of catalyst loading from 10 to 20 mg and further to 25 mg. But, the yield of the product did not increase further with 30 mg of **1'**. Hence, the optimum catalyst loading to achieve maximum conversion towards the product was fixed as 25 mg of **1'** at 100 °C after 20 h. The next parameter optimized for this condensation reaction was reaction temperature. The reaction was performed at 60, 80 and 120 °C under identical conditions. The conversion of **1** was significantly reduced (by two fold) upon decreasing the reaction temperature from 100 to 60 °C. On other hand, increasing the reaction temperature from 100 to 120 °C showed no changes in the conversion of **1** to the desired product. Also, the physical appearance of the catalyst changed at 120 °C. The observed catalytic data are plotted in Fig. 4. Hence, the optimum temperature to achieve the maximum conversion was fixed at 100 °C to retain catalyst structural integrity for further experiments.

In order to understand the nature of active sites, a series of control experiments were performed under identical conditions employed for **1'**. The activity of **1'** was compared with UiO-66(Hf) and free H₂-BDC-NH₂ linker with similar molar ratio present in **1'**. The observed catalytic results are shown in Fig. 5. These results clearly indicate that the activity of **1'** is slightly lower at initial reaction rate compared to free linker whereas the activity of UiO-66(Hf) is significantly lower than **1'** and free linker (Fig. 5). These catalytic data indicate that the superior activity of **1'** compared to UiO-66(Hf) is due to the presence additional BA sites in promoting this reaction.

Furthermore, the slightly higher activity of free organic linker than **1'** under identical reaction conditions is due to the presence of acidic/basic sites and the lack of diffusion limitations to reach these sites. Since these sites are located within the pores of **1'**, diffusion barrier is experienced by the reactants, thus affording lower initial activity. These results unambiguously prove that BA sites play an active role in promoting this condensation both in free linker and in **1'** than LA sites available in UiO-66(Hf). Furthermore, a control experiment was performed for the Friedländer condensation between **1** and **2** with pyridine under similar experimental conditions. The catalytic results indicated that the reaction rate and the conversion of **1** (8%) were significantly reduced upon addition of pyridine. These data show that the BA sites in the linker are quenched significantly by pyridine base, thus lowering the catalytic activity.

Interestingly, the activity of **1'** was compared with Cu₃(BTC)₂ under identical reaction conditions since the later catalyst was often employed as a preferred catalyst for this reaction.³⁸ The observed catalytic results indicate that Cu₃(BTC)₂ affords 95% yield after 6 h which is higher than that of **1'**.³⁸ However, the structural integrity of Cu₃(BTC)₂ underwent drastic change and it showed significant decrease of its activity in subsequent catalytic cycles.³⁸ This could be due to the possible reduction of Cu(II) sites at this reaction temperature. On other hand, the activity of **1'** was retained for prolonged use, thus implying the long term stability under these experimental conditions.

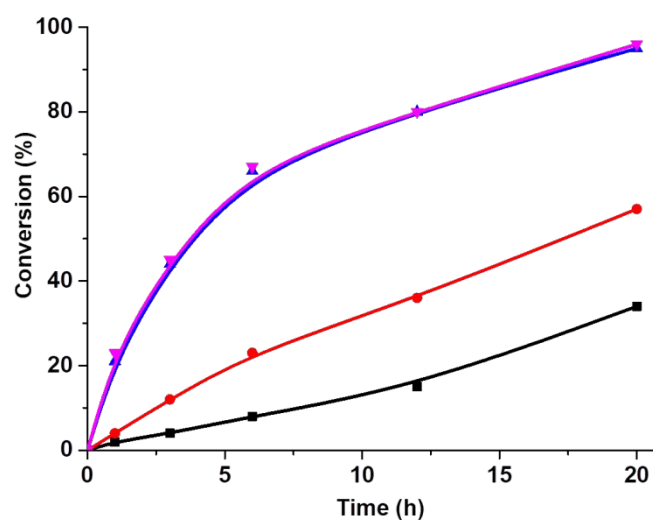


Fig. 4 Effect of temperature for the Friedländer condensation between substrate **1** and substrate **2** at (■) 60 °C, (●) 80 °C, (▲) 100 °C and (▼) 120 °C. The conversions are average of two independent experiments.

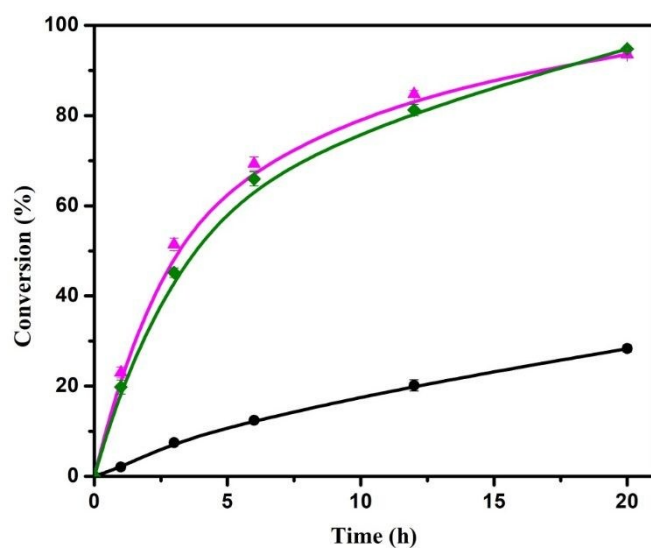


Fig. 5 Time conversion profiles for the Friedländer condensation between substrate 1 and substrate 2 using (■) UiO-66(Hf), (◆) 1' and (▲) H₂BDC-NHNH₂ linker with identical molar ratio to 1'.

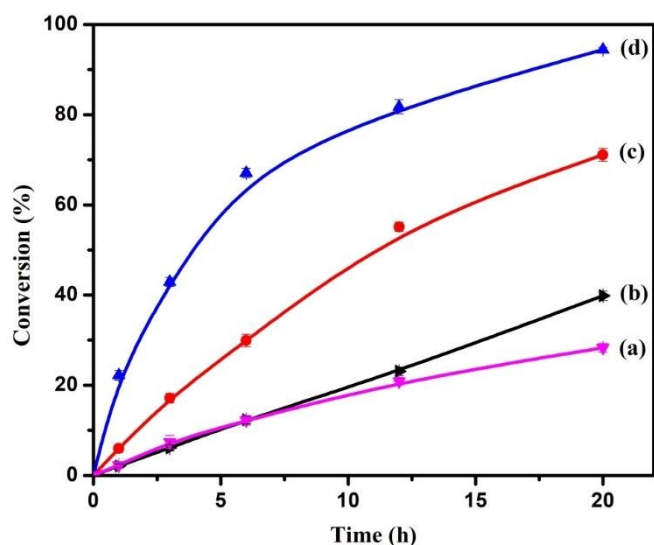


Fig. 6 Time conversion profiles for Friedländer condensation between substrate 1 and substrate 2 in the presence of (a) UiO-66(Hf), (b) UiO-66(Hf)-NH₂, (c) UiO-66(Zr)-NHNH₂ and (d) 1'.

Furthermore, the catalytic behavior of 1' was compared with analogous functionalized MOFs with basic sites like UiO-66(Hf), UiO-66(Hf)-NH₂ and UiO-66(Zr)-NHNH₂ in the Friedländer condensation between 1 and 2 under identical reaction conditions (Fig. 6). As predicted, the activity of UiO-66(Hf)-NH₂ was slightly higher than with UiO-66(Hf) solid and this is attributed to the presence of basic sites. In contrast, the activity of 1' is much higher than UiO-66(Hf) and UiO-66(Hf)-NH₂ and this superior activity of the former solid is due to the

existence of additional BA sites in 1' that plays an efficient role in promoting this condensation reaction. On other hand, the catalytic performance of 1' was notably higher than UiO-66(Zr)-NHNH₂ under similar conditions (Fig. 6). These differences in the activity between Hf and Zr MOFs with similar active sites may arise due to the lower pK_a of Hf MOFs than Zr MOFs.

One of the possible merits of developing heterogeneous solid catalysts for organic transformations is the facile separation of solid catalysts from the reaction mixture and subjecting it for subsequent cycles. Hence, this is one of the ways to ascertain catalyst stability under the reaction conditions. Therefore, the solid catalyst was removed after the catalytic reaction, washed, dried and reused in subsequent cycles. The observed catalytic data are shown in Fig. 7. These results imply that the solid maintains its catalytic performance up to four cycles with minimal decay in its activity and this loss is due to the catalyst loss during the recovery and reuse processes. To prove the catalyst stability further, XRPD patterns of the fresh, recovered and four times used solid catalysts were measured and the observed XRPD patterns are shown in Fig. 8. Comparison of these XRPD patterns of the fresh and four times used solids unambiguously confirm that the structural integrity and peak intensities are well preserved during the catalytic reaction (Fig. 8) which are reflected in the reusability, leaching and ICP-AES analysis. To support these claims further, EDX and FE-SEM studies were carried out. The EDX elemental spectrum and mapping analyses (Figs. S2-S5, ESI⁺) after the 4th catalytic cycle confirmed that the presented catalyst preserved the elements present in it before the catalysis (Hf, C, O and N). The FE-SEM analyses (Figs. S6-S7, ESI⁺) after the 4th catalytic cycle also confirmed the surface morphology (octahedral shape) remained similar to the fresh solid.

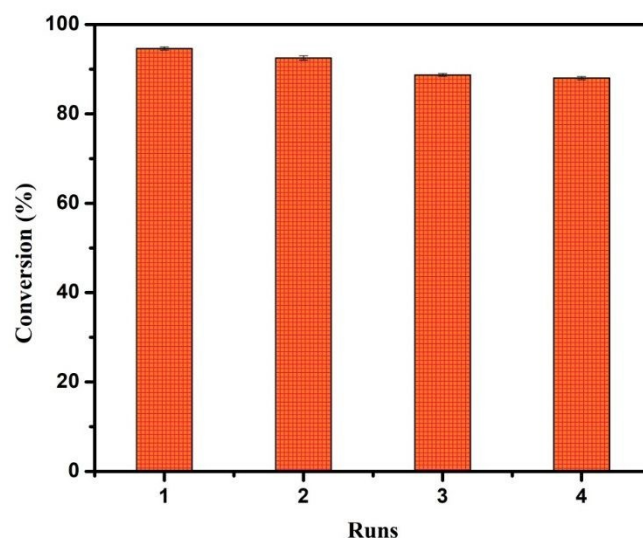


Fig. 7. Reusability profile for the Friedländer condensation between substrate 1 and substrate 2 employing 1' as heterogeneous solid base catalyst.

Although many catalytic systems have been reported for this transformation, the active sites promoting this reaction were mainly unsaturated coordination sites. For example, a high population of active sites in $\text{Cu}_3(\text{BTC})_2$ together with the concerted effect of the presence of a pair of adjacent coordinatively unsaturated Cu^{2+} sites was responsible for promoting this condensation reaction.^{2, 38, 46-50} In addition, a continuous flow process was also developed for this condensation reaction using $\text{Cu}_3(\text{BTC})_2$ as heterogeneous solid Lewis acid catalyst employing unsaturated Cu^{2+} sites.⁵¹ In another precedent, Cu-doped ZIF-8 (Cu/ZIF-8) material exhibited higher catalytic activity in Friedländer condensation due to its higher surface area and high dispersion of Cu^{2+} sites over ZIF-8 with easy accessibility by reactants.⁵² Therefore, some of the salient features of this work are the use of dual functional MOF to promote this condensation, employment of Hf(IV)-based solids rather than Cu(II) as active sites and wide substrate scope compared to earlier reported data.^{2, 38, 47, 51}

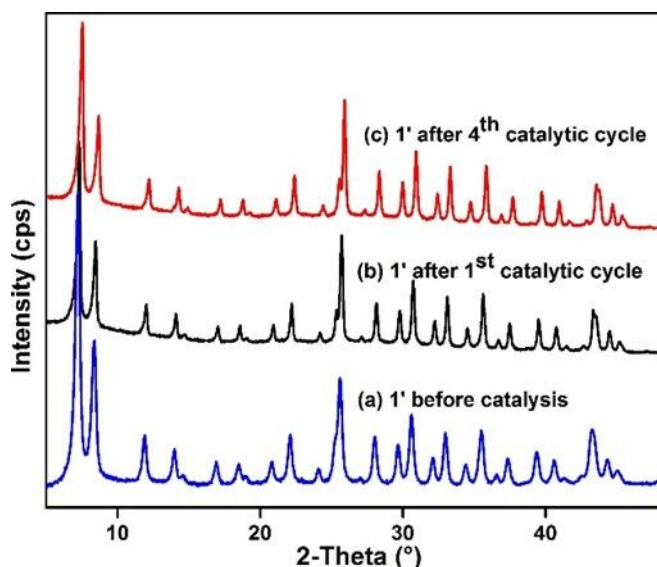


Fig. 8 XRPD patterns of 1' (a) before catalysis, (b) recovered after one cycle and (c) recovered after four cycles.

Table 1. Friedländer condensation between different 2-aminoaryl ketones and active methylene compounds using 1' as a solid base catalyst.^a

Entry	2-Aminoaryl Ketones	Active Methylene Compounds	Product	Conversion ^b (%)
1				95
2				94
3				68
4				98
5				98
6				84
7				81
8				100 (60:40)
9				100 (48:52)
10				98

^a Reaction conditions: 2-aminoaryl ketones (0.5 mmol), active methylene compounds (0.3 mL), 1' (25 mg), 100 °C, 20 h.

^b Conversion of 2-aminoarylketone was determined by GC using internal standard method. The conversions are provided with the average of two experiments.

One of the main objectives of this work is to demonstrate the feasibility of this catalyst to screen wide range of substrates towards the synthesis of quinoline derivatives with different ketones and active methylene compounds. Although many MOF based catalysts have been reported for this transformation, many of them suffer with substrate scope and only very few works have attempted to obtain series of quinolines. After optimizing the reaction conditions, the catalytic behavior of **1'** was checked with wide varieties of substrates and the observed results are shown in Table 1. Under the optimized reaction conditions, **1** and **2** afforded 95% conversion of the desired product with **1'** as solid catalyst. Further, 2-amino-5-chlorobenzophenone readily reacted with **2** to afford the desired quinoline derivative at 94% conversion. On other hand, 2-amino-5-nitrobenzophenone reacted with **2** at 68% conversion to its respective product under identical conditions. This lower conversion may be due to the electron withdrawing nature of nitro by reducing the electron density in amino group. Further, 2-(4-chlorobenzoyl)aniline and 2-(4-bromobenzoyl)aniline were reacted with **2** at quantitative conversions under similar conditions using **1'** as solid catalyst. Furthermore, 2-aminoacetophenone was smoothly condensed with dimethylmalonate in the presence of **1'** at 84% conversion to the desired product. A similar trend was also observed for the reaction of 2-aminoacetophenone with diethylmalonate. In addition, mixture of products were observed for the condensation between 2-aminoacetophenone with methylacetoacetate and ethylacetoacetate under similar reaction conditions. Finally, 2-aminoacetophenone was smoothly condensed with cyclohexanone using **1'** as solid catalyst at 98% conversion under similar conditions.

Conclusions

To summarize, the Hf-Uio66-N₂H₃ MOF was synthesized via the reported solvothermal method and characterized completely. The guest free form (**1'**) of the as-synthesized material (**1**) was judiciously tested as a catalyst in modified Friedländer synthesis. The catalyst **1'** was capable of efficiently performing the synthesis of 3-acetyl-2,4-dimethylquinoline through Friedlander condensation of 2-aminoacetophenone and acetylacetone as starting materials. It also showed wide substrate scope and high conversions to the desired products. The catalyst was stable up to four catalytic cycles without decreasing its catalytic efficiency. A sequence of control experiments was performed where the presented catalyst showed the best catalytic performance. Finally, this encouraging catalytic performance suggests that new catalysts can be developed by judicious design of functionalized MOFs.

Acknowledgements

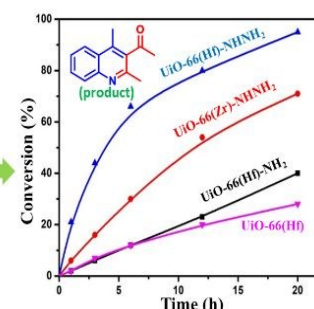
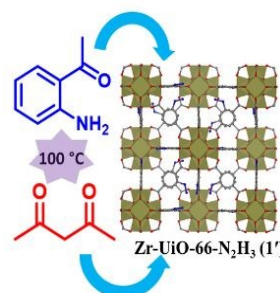
Financial assistance from Science and Engineering Research Board, New Delhi, is thankfully acknowledged via grant no. EEQ/2016/000012 and EMR/2016/006500 for SB and AD, respectively. AD thanks the University Grants Commission, New Delhi, for the award of an Assistant Professorship under its Faculty Recharge Programme.

Notes and references

- J. Marco-Contelles, E. Pérez-Mayoral, A. Samadi, M. d. C. Carreiras and E. Soriano, *Chem. Rev.*, 2009, **109**, 2652–2671.
- E. Pérez-Mayoral, Z. Musilová, B. Gil, B. Marszalek, M. Položij, P. Nachtigall and J. Čejka, *Dalton Trans.*, 2012, **41**, 4036–4044.
- A. V. Malkov, M. A. Kabeshov, M. Bella, O. Kysilka, D. A. Malyshev, K. Pluháčková and P. Kočovský, *Org. Lett.*, 2007, **9**, 5473–5476.
- H. Naruto and H. Togo, *Org. Biomol. Chem.*, 2019, **17**, 5760–5770.
- N. Anand, S. Koley, B. J. Ramulu and M. S. Singh, *Org. Biomol. Chem.*, 2015, **13**, 9570–9574.
- X.-F. Shang, S. L. Morris-Natschke, Y.-Q. Liu, X. Guo, X.-S. Xu, M. Goto, J.-C. Li, G.-Z. Yang and K.-H. Lee, *Med. Res. Rev.*, 2019, **38**, 775–828.
- J. P. Michael, *Nat. Prod. Rep.*, 2008, **25**, 166–187.
- J. Xu, J. Sun, J. Zhao, B. Huang, X. Li and Y. Sun, *RSC Adv.*, 2017, **7**, 36242–36245.
- D. Kumar, A. Kumar, M. M. Qadri, M. I. Ansari, A. Gautam and A. K. Chakraborti, *RSC Adv.*, 2015, **5**, 2920–2927.
- K. Hu, C. Liu, J. Li and F. Liang, *Med. Chem. Commun.*, 2018, **9**, 1663–1672.
- S. Kondaparla, A. Soni, A. Manha, K. Srivastava, S. K. Puri and S. B. Katti, *RSC Adv.*, 2016, **6**, 105676–105689.
- J. J. Eisch and T. Dluzniewski, *J. Org. Chem.*, 1989, **54**, 1269–1274.
- N. P. Buu-Hoi, R. Royer, N. D. Xuong and P. Jacquignon, *J. Org. Chem.*, 1953, **18**, 1209–1224.
- H. R. Henze and D. W. Carroll, *J. Am. Chem. Soc.*, 1954, **76**, 4580–4584.
- J. C. Sloop, *J. Phys. Org. Chem.*, 2009, **22**, 110–117.
- S. Jain, V. Chandra, P. K. Jain, K. Pathak, D. Pathak and A. Vaidya, *Arabian J. Chem.*, 2016, **12**, 4920–4946.
- D. K. T. Yadav and B. M. Bhanage, *RSC Adv.*, 2015, **5**, 51570–51575.
- R. K. Saunthwal, M. Patel and A. K. Verma, *J. Org. Chem.*, 2016, **81**, 6563–6572.
- J. Akbari, A. Heydari, H. R. Kalhor and S. A. Kohan, *J. Comb. Chem.*, 2010, **12**, 137–140.
- B. W. J. Chen, L. L. Chng, J. Y. Y. Wei, J. Yang and J. Y. Ying, *ChemCatChem*, 2013, **5**, 277–283.
- M. K. Barman, A. Jana and B. Maji, *Adv. Synth. Catal.*, 2018, **360**, 3233–3238.
- M. Mastalir, M. Glatz, E. Pittenauer, G. Allmaier and K. Kirchner, *J. Am. Chem. Soc.*, 2016, **138**, 15543–15546.
- M. Jafarzadeh, E. Soleimani, P. Norouzi, R. Adnan and H. Sepahvand, *J. Fluorine Chem.*, 2015, **178**, 219–224.
- V. F. Batista, D. C. G. A. Pinto and A. M. S. Silva, *ACS Sustainable Chem. Eng.*, 2016, **4**, 4064–4078.

25. B. Gole, A. K. Bar and P. S. Mukherjee, *Chem. Commun.*, 2011, **47**, 12137-12139.
26. B. Gole, A. K. Bar and P. S. Mukherjee, *Chem. - Eur. J.*, 2014, **20**, 13321-13336.
27. A. Karmakar, P. Samanta, A. V. Desai and S. K. Ghosh, *Acc. Chem. Res.*, 2017, **50**, 2457-2469.
28. R. Goswami, N. Seal, S. R. Dash, A. Tyagi and S. Neogi, *ACS Appl. Mater. Interfaces*, 2019, **11**, 40134-40150.
29. S. Sen, N. N. Nair, T. Yamada, H. Kitagawa and P. K. Bharadwaj, *J. Am. Chem. Soc.*, 2012, **134**, 19432-19437.
30. D. De, T. K. Pal, S. Neogi, S. Senthilkumar, D. Das, S. S. Gupta and P. K. Bharadwaj, *Chem. - Eur. J.*, 2016, **22**, 3387-3396.
31. B. Parmar, P. Patel, V. Murali, Y. Rachuri, R. I. Kureshy, N.-U. H. Khan and E. Suresh, *Inorg. Chem. Front.*, 2018, **5**, 2630-2640.
32. P. Patel, B. Parmar, R. S. Pillai, A. Ansari, N.-U. H. Khan and E. Suresh, *Appl. Catal.*, A, 2020, **590**, 117375-117382.
33. A. C. Dreischarf, M. Lammert, N. Stock and H. Reinsch, *Inorg. Chem.*, 2017, **56**, 2270-2277.
34. A. S. Abou-Elyazed, G. Ye, Y. Sun and A. M. El-Nahas, *Ind. Eng. Chem. Res.*, 2019, **58**, 21961-21971.
35. H. Zhang, X.-W. Gao, L. Wang, X. Zhao, Q.-Y. Li and X.-J. Wang, *CrystEngComm*, 2019, **21**, 1358-1362.
36. M. Rimoldi, A. J. Howarth, M. R. DeStefano, L. Lin, S. Goswami, P. Li, J. T. Hupp and O. K. Farha, *ACS Catal.*, 2017, **7**, 997-1014.
37. S. Rojas-Buzo, P. García-García and A. Corma, *Green Chem.*, 2018, **20**, 3081-3091.
38. E. Pérez-Mayoral and J. Čejka, *ChemCatChem*, 2011, **3**, 157-159.
39. X.-Y. Zhou, X. Chen and L.-G. Wang, *Synth. Commun.*, 2018, **48**, 830-837.
40. M. H. Beyzavi, R. C. Klet, S. Tussupbayev, J. Borycz, N. A. Vermeulen, C. J. Cramer, J. F. Stoddart, J. T. Hupp and O. K. Farha, *J. Am. Chem. Soc.*, 2014, **136**, 15861-15864.
41. A. Das, N. Anbu, A. Dhakshinamoorthy and S. Biswas, *Microporous Mesoporous Mater.*, 2019, **284**, 459-467.
42. Y. Liu, R. C. Klet, J. T. Hupp and O. Farha, *Chem. Commun.*, 2016, **52**, 7806-7809.
43. G. C. Shearer, S. Chavan, S. Bordiga, S. Svelle, U. Olsbye and K. P. Lillerud, *Chem. Mater.*, 2016, **28**, 3749-3761.
44. C. A. Clark, K. N. Heck, C. D. Powell and M. S. Wong, *ACS Sustainable Chem. Eng.*, 2019, **7**, 6619-6628.
45. K. Y. Cho, J. Y. Seo, H.-J. Kim, S. J. Pai, X. H. Do, H. G. Yoon, S. S. Hwang, S. S. Han and K.-Y. Baek, *Applied Catalysis B: Environmental*, 2019, **245**, 635-647.
46. Z.-W. Zhai, S.-H. Yang, M. Cao, L.-K. Li, C.-X. Du and S.-Q. Zang, *Cryst. Growth Des.*, 2018, **18**, 7173-7182.
47. W.-Y. Gao, K. Leng, L. Cash, M. Chrzanowski, C. A. Stackhouse, Y. Sun and S. Ma, *Chem. Commun.*, 2015, **51**, 4827-4829.
48. N. T.S.Phan, T. T.Nguyen, K. D.Nguyen and A. X.T.Vo, *Appl. Catal.*, A, 2013, **464-465**, 128-135.
49. V. Sharma, D. De and P. K. Bharadwaj, *Inorg. Chem.*, 2018, **57**, 8195-8199.
50. A. K. Gupta, D. De and P. K. Bharadwaj, *Dalton Trans.*, 2017, **46**, 7782-7790.
51. A. Sachse, R. Ameloot, B. Coq, F. Fajula, B. Coasne, D. D. Vos and A. Galarneau, *Chem. Commun.*, 2012, **48**, 4749-4751.
52. A. Schejn, A. Aboulaich, L. Balan, V. Falk, J. Lalevé, G. Medjahdi, L. Aranda, K. Mozet and R. Schneider, *Catal. Sci. Technol.*, 2015, **5**, 1829-1839.

Table of Content (TOC):



A hydrazine functionalized Hf MOF was employed as a heterogeneous catalyst for synthesis of quinolone scaffold with high yields. The catalyst showed broad substrate scope and excellent recyclability.